Available online at www.sciencedirect.com
SCIENCE DIRECT
International Journal of Heat and Fluid Flow 27 (2006) 644–652
International Journal of HEAT AND FLUID FLOW
www.elsevier.com/locate/ijhff

The role of nonlinearity in turbulent diffusion models for stably stratified and rotating turbulence

L. Liechtenstein *, F.S. Godeferd, C. Cambon

Laboratoire de Mécanique des Fluides et d'Acoustique UMR 5509, ECL-UCB-CNRS, 36, Avenue Guy de Collongue, 69131 Ecully Cedex, France

Available online 30 March 2006

Abstract

Dispersion in rotating and stratified turbulence is investigated by an analytical linear model, kinematic simulations and direct numerical simulations in order to observe the impact of nonlinearity on single-particle and two-particle statistics. The anisotropy of these Lagrangian quantities is discussed in relation with the Eulerian field anisotropy and its structures, pancake- or cigar-shaped depending on the dominant body force. We show that a linear approach is valid for single-particle dispersion, and that the nonlinear structuring of the Eulerian field influences particle dispersion at long times.

Keywords: Turbulence; Rotation; Stratification; Single-particle dispersion; Two-particle dispersion; Kinematic simulation

1. Introduction

Lagrangian models of rotating and stratified turbulence are needed to model mixing and transport in geophysical flows. Environmental applications, such as the simulation of dispersion of pollutants from a planned industrial facility or the transport of nutrients in the ocean are actual problems which need an accurate Lagrangian model of rotating and stratified turbulence. Furthermore, mixing of chemicals in environmental flows, such as ozone in the atmosphere or carbon dioxide in the ocean can have strong climatic effects due to different rates of the associated chemical reactions. Simulations of these processes necessitate a good understanding of the Lagrangian processes in rotating stratified turbulence.

Experimental Lagrangian data or measurements in nature are rare (Richardson, 1926) as following fluid particles in a turbulent flow is difficult. How can we simplify geophysical flows to capture main physical mechanisms without the influence of secondary effects? We choose to analyse homogeneous, strongly stratified and rapidly rotating turbulence. It is definitely too far removed from applications to be quantitatively compared with them. However, as the role of turbulence with its nonlinear interactions in geophysical systems is barely known, we believe that this simplified system can add valuable qualitative insights into the nonlinear mechanisms of geophysical turbulence. This physical understanding of the nonlinear mechanisms will be of vital importance, if one wants to start to model more complex geophysical applications.

One method of gaining information on turbulent diffusion is to find and apply laws connecting the Eulerian and Lagrangian velocity fields and calculate Lagrangian statistics with Eulerian velocity fields. Stable stratification and rotation is taken into account in the Boussinesq system of equations

$$\partial_t \boldsymbol{u} + \boldsymbol{u}\cdot\nabla\boldsymbol{u} - \nu\nabla^2\boldsymbol{u} = -\nabla p - 2\Omega\boldsymbol{n}\times\boldsymbol{u} + b\boldsymbol{n}, \tag{1}$$

$$\partial_t b + \boldsymbol{u}\cdot\nabla b - \chi\nabla^2 b = -N^2\boldsymbol{n}\cdot\boldsymbol{u}, \tag{2}$$

$$\nabla\cdot\boldsymbol{u} = 0 \tag{3}$$

with N the Brunt–Vaisala (buoyancy) frequency and Ω the rotational frequency. Both parameters act on the velocity field linearly and compete against the nonlinear advection term. Furthermore, for cases with rotation and stratifica-

* Corresponding author.
E-mail address: llukas@gmail.com (L. Liechtenstein).

0142-727X/$ - see front matter © 2006 Elsevier Inc. All rights reserved.
doi:10.1016/j.ijheatfluidflow.2006.02.010

tion, the ratio of $\alpha = 2\Omega/N$ is a crucial non-dimensional number characterizing the flow.

"Turbulence" and "wave" like dynamics are defined by splitting the velocity field in the eigenmodes of the linearized system (1)–(3), so that the total turbulent energy of a rotating and stratified flow can be divided into a vortex mode and a wave mode. The vortex mode is a fraction of the horizontal velocity field, storing kinetic energy. Its linear evolution is time independent. The wave mode consists partly of the non-vortex velocity field, also storing kinetic energy, and the buoyancy field, storing potential energy. The linear evolution of the wave mode is governed by the dispersion relation $\sigma = \sqrt{N^2 \sin^2\theta + 4\Omega^2 \cos^2\theta}$ which depends on θ, the polar angle with the vertical. It creates a singular case for the value $\alpha = 1$, as a limit between the rotation dominant from the stratification dominant cases. Linear processes in the flow field differ over the cases, due to linear wave dynamics with variable dispersion laws.

Lagrangian statistics are basically generated by following particles, in our case equivalent to fluid elements, in a velocity field and by calculating statistics of the position as a function of time. Statistics means the average over values of all trajectories and/or ensembles with notation $\langle\ \rangle$.

The Lagrangian frame of reference is moving with a fluid element, so fundamentally different from the Eulerian one. The initial particle position is important, as it is the decisive quantity deciding the evolution of the trajectory. The Lagrangian position of a fluid element labeled by the initial position $\boldsymbol{X}$, $\boldsymbol{x}(t) = \boldsymbol{x}(\boldsymbol{X}, t)$, has a Lagrangian velocity $\boldsymbol{V}(t)$ related to the Eulerian velocity field $\boldsymbol{u}(x, t)$ by $\boldsymbol{V}(t) = \boldsymbol{u}(\boldsymbol{x}(\mathbf{X}, t), t)$. Therefore the position of the particle advected by the Lagrangian velocity field can be written as

$$\dot{\boldsymbol{x}}(t) = \boldsymbol{V}(\boldsymbol{X}, t) = \boldsymbol{u}(\boldsymbol{x}(\boldsymbol{X}, t), t), \tag{4}$$

which subjects the Lagrangian position of the particle $\boldsymbol{x}(t)$ to feedback by itself and consequently to a nonlinear evolution.

We study two Lagrangian quantities, the first of which is single-particle dispersion, i.e. the time evolution of the distance particles have from their initial position $\boldsymbol{X}$. Second, we also calculate relative dispersion defined as two-particle dispersion, i.e. the time evolution of the distance between two initially neighbouring particles.

1.1. The role of nonlinear processes in Lagrangian statistics

The trajectory equation (4) is nonlinear. Is this enough to model advective properties of a time-dependent flow field? Is a linear flow field enough to model Lagrangian statistics without using trajectories and therefore Eq. (4)? The role of nonlinearity in the dynamics of the flow field on Lagrangian statistics is a key point in answering this question. In Fig. 1 we show trajectories integrated in a velocity field obtained with a nonlinear method (top) and a linear

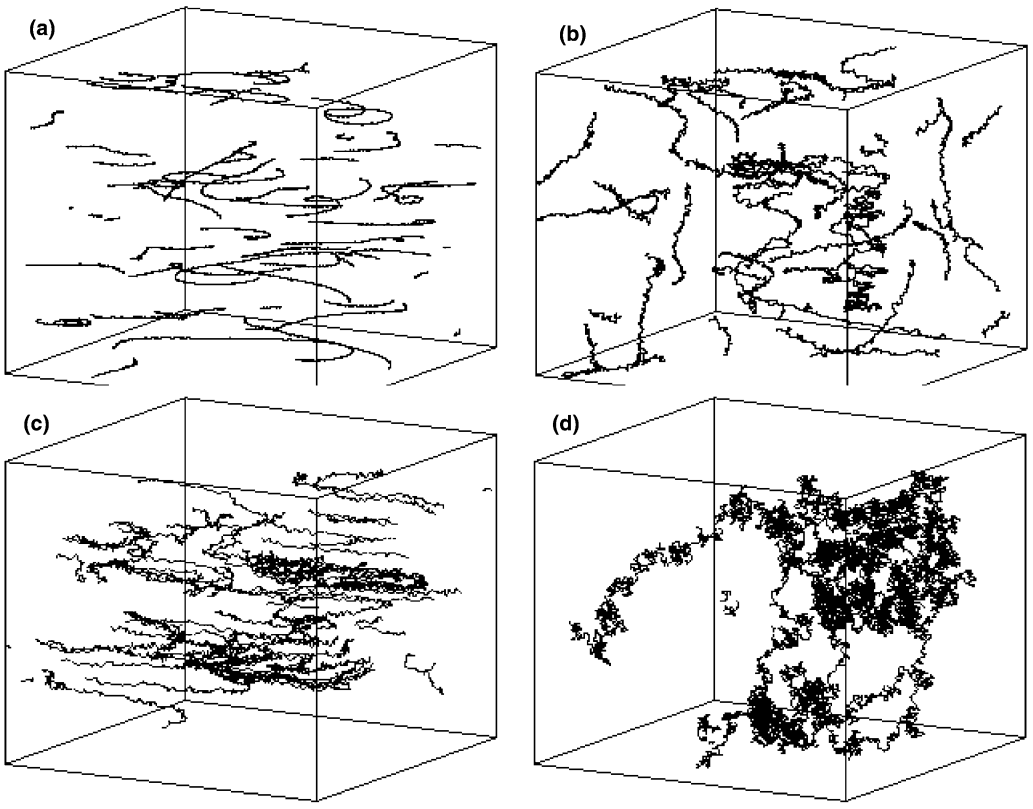

Fig. 1. Examples of trajectories in anisotropic turbulence integrated in different velocity fields: (a) nonlinear stratified, (b) nonlinear rotating, (c) linear stratified and (d) linear rotating.

model (bottom). Qualitatively, the trajectories look different. However, a quantitative analysis of the statistics of these trajectories lead to different conclusions.

Taylor (1921) discovers a relationship between Lagrangian velocity correlations and one-particle dispersion, but, with an argument of Corrsin (1963), a model of one-particle dispersion can be developed in the framework of Rapid Distortion theory (RDT) (Cambon and Scott, 1999), from Eulerian two-time velocity correlations (Cambon et al., 2004). This linear model manages to quantitatively predict velocity correlations and single-particle dispersions for rotating and stratified turbulence for moderate times. At long times, when diffusion processes dominate, the model is expected to be inaccurate. Nevertheless, the importance of nonlinear processes in Lagrangian statistics where only one trajectory is involved seems limited. This might change for two-particle dispersion. Preliminarily, we found the role of nonlinearity in stratified and rotating Lagrangian statistics relatively unimportant, especially when one compares this role to the one in Eulerian statistics.

So how can one distinguish linear from nonlinear phenomena in a simple way? We use results for Lagrangian quantities obtained with three fundamentally different approaches. The first method uses two-time velocity correlation functions analytically deduced with RDT. They are put into relation with Lagrangian statistics using the simplified Corrsin hypothesis. This method is therefore strictly linear, using no integration of Lagrangian trajectories and is referred to as "RDT/SCH".

Trajectories integrated with the help of kinematic simulations (KS) are used to simulate the properties of Lagrangian statistics. KS uses an ensemble of frozen vector fields, composed of random spatial Fourier modes, as velocity fields. The trajectories are therefore followed on these spatially random velocity fields which incorporate the exact linear wave dynamics. Thus, the intrinsic nonlinearity of the trajectory equation (4) has an effect on Lagrangian statistics.

The third method consists in tracking particles within velocity fields generated by fully nonlinear direct numerical simulations (DNS). So all dynamical nonlinearities as well as any nonlinearities from the trajectory equation (4) are taken into account.

1.1.1. Linear Lagrangian model: RDT/SCH

The possibility of evaluating velocity correlations at arbitrary times from RDT in connection with Taylor's relation (Taylor, 1921), suggests a model to predict single-particle dispersion (Cambon et al., 2004) relating Eulerian and Lagrangian velocity correlations by a simplified Corrsin hypothesis (SCH) (Kaneda and Ishida, 2000; Corrsin, 1963).

Provided the initial velocity field is known, the exact linear solution from RDT not only yields the time evolution of the velocity field $\hat{\boldsymbol{u}}$ but also analytical expressions for higher-order single-point statistics, upon integration of two-point correlations of $\hat{\boldsymbol{u}}$ in spectral space. This yields kinetic energy spectra, potential energy, and two-point two-time spectra of the horizontal or vertical velocity components. Strictly speaking, this method only applies to Eulerian correlation spectra but, following Corrsin's argument, these can replace Lagrangian ones when computing single-particle dispersion with the time integration method of Taylor (Eq. (6)). This gives an analytical expression for calculating one-particle Lagrangian displacement correlations using two-time velocity correlations (Kaneda and Ishida, 2000; Cambon et al., 2004). Details of the method are explained in Cambon et al. (2004), which also describes the general results for the stratified/rotating case with arbitrary initial partition of potential and kinetic energies. In these results, we observe that the mere variation of dispression relation due to different cases produces different dispersion behaviours of the linear model.

1.1.2. Kinematic simulation

Kinematic simulation models a turbulent velocity field as a superposition of *random Fourier modes* so that the field is automatically incompressible. No dynamical equation is involved, although oscillations physically related to internal waves are explicitly introduced for each mode by using the linear solution from RDT (Nicolleau and Vassilicos, 2000).

Both the choice of random wave vectors distribution and the initialization of KS need to be done with extreme care to render it as physically realistic as possible, as no dynamic processes alter the initial field later on. Once this is properly taken care of, Lagrangian statistics calculated with KS capture the main Lagrangian properties of anisotropic turbulence.

In KS, the time-dependent velocity field $\hat{u}^{(i)}(\boldsymbol{k})$ is expressed in the Craya–Herring frame of reference (spectral unit vectors $e^{(1)}$ and $e^{(2)}$ which ensure incompressibility, see Liechtenstein et al., 2005), as a discrete Fourier sum

$$u_i(\boldsymbol{x},t) = \sum_{(n,m)=(1,1)}^{(m,n)=(M_\theta,N_k)} \left(\hat{u}^{(1)}_{mn}(t)e^{(1)}_{mn;i} + \hat{u}^{(2)}_{mn}(t)e^{(2)}_{mn;i}\right)\mathrm{e}^{\mathrm{i}\boldsymbol{k}_{mn}\cdot\boldsymbol{x}} \qquad (5)$$

where the subscript mn implies a dependence on the discretized wave vector $\boldsymbol{k}_{mn}$ which alone represents a given wave number at a given polar angle θ_m. The total number of resolved modes is $N_k M_\theta = 10{,}000$ with $N_k = 25$ and $M_\theta = 400$.

The time evolution of $\hat{u}^{(i)}(\boldsymbol{k}_{mn},t)$ is given by the discrete RDT linear solution, which propagates the chosen initial conditions obtained by computing the Green's function of the linearized system (1)–(3).

KS is then used as a Lagrangian model of turbulent diffusion by numerically solving the fluid trajectory equation (4), where the velocity $\boldsymbol{u}(\boldsymbol{x})$ is given by (5).

The spectral energy distribution is fixed throughout the time by an analytically prescribed standard spectrum ($\propto k^4$ for $k_{\min} < k < k_i$ and ($\propto k^{-2.5}$ for $k_i < k < k_{\max}$). The different runs of KS with their denomination and a few parameters including a Reynolds number defined as $Re_k = k_{\max}/k_i$ are shown in Table 1.

Table 1
Some parameters of KS

	N	2Ω	α	Re_k	q	k_i
KS0	30π	0	0	100	1	1
KS0.1	30π	3π	0.1	100	1	1
KS1	30π	30π	1	100	1	1
KS10	3π	30π	10	100	1	1
KSinf	0	30π	∞	100	1	1

Table 2
Some parameters of DNS

	N	2Ω	α	Re_λ	q	L
DNS0	10π	0	0	130	0.6	0.3
DNS0.1	10π	π	0.1	130	0.6	0.3
DNS1	10π	10π	1	100	0.6	0.25
DNS10	π	10π	10	170	0.6	0.3
DNS-inf	0	10π	∞	170	0.6	0.3
DNS-iso	0	0	–	90	0.4	0.25

1.1.3. Direct numerical simulation

Direct numerical simulation is used to solve the Boussinesq Equations (1)–(3) with a standard fully de-aliased pseudo-spectral collocation method permitted by homogeneity (Rogallo, 1981). Trajectories are followed through the flow field in order to generate Lagrangian statistics. Although the initialization is less important in DNS than KS, as triadic exchanges slowly de-correlate the velocity field from the initial fields, transient effects due to an anisotropic initialization sometimes disappear only after several turbulent turnover times. We initialize using isotropic initial conditions and a narrow band initial energy spectrum, and a resolution of 512^3 points is used. No forcing is implemented, meaning that the turbulence in the DNS is freely decaying. To let higher-order velocity correlations grow, we perform an isotropic pre-calculation, and thereby allow for discontinuities in statistical data derivatives at the time of introduction of an anisotropic body force into the system.

In the second method, trajectories in DNS are obtained by solving the fluid trajectory equation (4) as for KS. Some initial parameters from the runs of the DNS are shown in Table 2, including the Reynolds number based on the Taylor microscale Re_λ.

2. Single-particle dispersion

A basic Lagrangian quantity is the single-particle dispersion. By integration along the trajectory of a fluid element, one gets mean displacements along each ith direction $\Delta x_i(t,t') = x_i(t) - x_i(t') = \int_{t'}^{t} \dot{x}_i(s)\mathrm{d}s$, which as covariances, give single-particle dispersion in all three space directions, $i = 1,2,3$ (Taylor, 1921)

$$\Delta_{ii}(t,t') = \langle \Delta x_i(t,t') \rangle^2 = \int_{t'}^{t} \mathrm{d}s' \int_{t'}^{t} \langle \dot{x}_i(s)\dot{x}_i(s') \rangle \mathrm{d}s. \qquad (6)$$

7200 particle pairs are interpolated in each run of the KS, while 2500 particle pairs are traced in each run of the DNS. For the analytical linear method, the Lagrangian velocity correlations in (6) are replaced by their Eulerian counterparts derived from RDT (Cambon et al., 2004), following the simplified Corrsin hypothesis.

For studying anisotropy, we compare single-particle dispersion in the horizontal and the vertical directions separately.

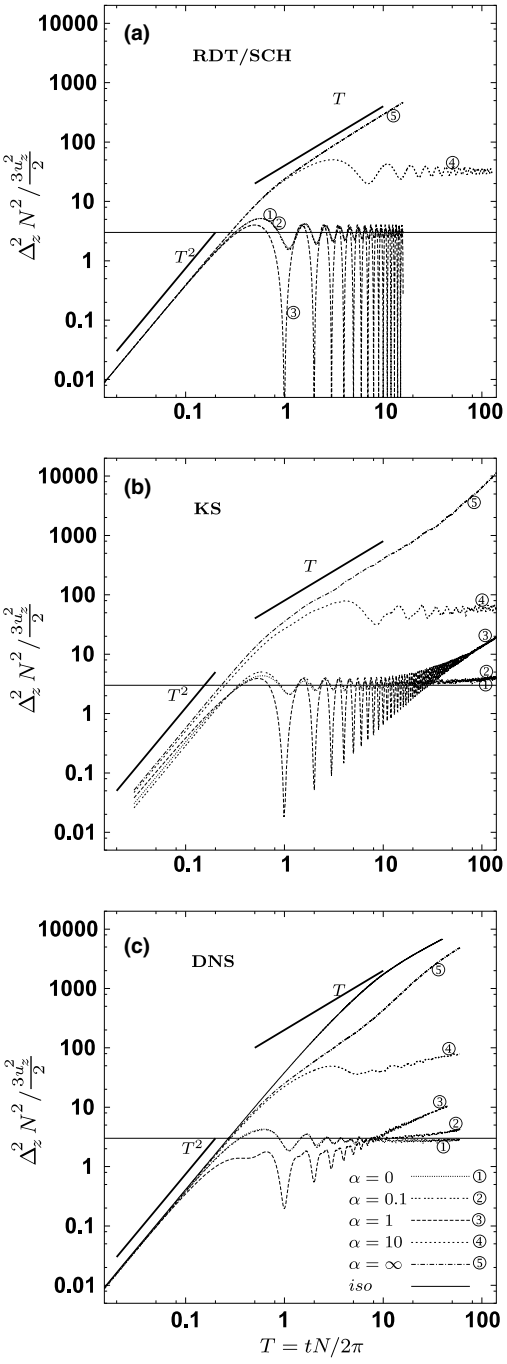

Fig. 2. (a) Linear prediction, (b) KS, and (c) DNS of vertical single-particle dispersion for different $\alpha = 2\Omega/N$. The dominantly rotating curves are scaled with 2Ω instead of N for the time as well as the dispersion scale. The horizontal lines show the value 3 of the plateau.

2.1. Vertical single-particle dispersion

Vertical single-particle dispersion $\Delta_{33}(0,t)$ is shown in Fig. 2 calculated with RDT/SCH, KS and DNS. The similarity of the three figures is remarkable, considering the differences in the methods with which the results have been obtained. Especially the statistics obtained from KS and DNS are remarkably similar.

Four phenomena may be identified:

- A ballistic regime ($\Delta_{33} \propto t^2$) can be observed at small times, for all the values of α and all models.
- An oscillating plateau for cases with non-zero stratification, even if rotation is dominant, is seen at intermediate or long times.
- For rotating cases, linear $\Delta_{33} \propto t$ laws can be observed at intermediate times.
- Finally, at longer times a Brownian regime can be observed for some cases, such that $\Delta_{33} \propto t$.

The ballistic regime is expected in all Lagrangian dispersions, illustrating simply the absence of interactions between the fluid particle and the flow for small enough times. It defines the smallest Lagrangian time scale, measuring the time at which the flow starts to interact with the fluid particle. For the vertical particle dispersion in rotating and stratified turbulence, this time can be universally normalized by using T as the time scale. The ballistic regime is observed up to around $T = 0.5$, similar in all cases, as it is a linear phenomenon. The absolute values of the one-particle dispersion can be normalized by the dominating parameter N or 2Ω, and by the initial vertical turbulent kinetic energy $\langle u_z^2 \rangle/2$ (Nicolleau and Vassilicos, 2000). For an isotropic Reynolds stress tensor, such as in RDT/SCH, this comes down to using the total turbulent kinetic energy $q^2/2 = \langle u_x^2 + u_y^2 + u_z^2 \rangle/2$, but in DNS, due to its anisotropic velocity field, the differences can be large. In KS, the anisotropy in the turbulent kinetic energy has no effect and $q^2/2$ is used as normalization.

The plateaus illustrate a confinement of vertical displacements for fluid particles, which scale with any non-zero value of N. This plateau is definitive in RDT/SCH, while it disappears for KS and DNS at long times. The scaling of the plateau universally fixes the evolution for the vertical one-particle dispersion (Nicolleau and Vassilicos, 2000), and, apart from the purely rotating regime with $\alpha = \infty$, the scaling seems to be always valid, even for dominant rotating cases. The horizontal lines in Fig. 2 are plotted for an absolute value of 3, indicating that the vertical dispersion scales with $\langle u_z^2 \rangle/2$ rather than with $q^2/2$. The nonlinear phenomena in Lagrangian statistics develop on a long-time scale, so the absolute confinement of particles in the vertical one-particle dispersion is a linear effect. The absolute confinement is a consequence of the potential energy which can be transformed to kinetic energy, limited for each fluid particle. However, if the available potential energy varies, the confinement can be replaced by a diffusive motion which would exhibit a Brownian T-law. Such an effect needs diffusive mechanisms for the scalar, in our case density fluctuations. Although the available potential energy is fixed for an instant in time, it can "regain" lost potential energy by nonlinear transfers from neighbouring fluid particles.

The Brownian regime is a typical phenomenon observed in one-particle dispersion in isotropic turbulence. At some distance $\Delta \boldsymbol{x}$ from the particle's initial position, the Lagrangian velocities at the initial and current positions are uncorrelated so that the increase in $\Delta \boldsymbol{x}$ follows a random-walk. $\Delta \boldsymbol{x}$ is therefore Brownian and follows a $(\Delta \boldsymbol{x})^2 \propto T$ law observed in Fig. 2(c) for the run DNS-iso at $T \approx 10$. The time associated with this transition is associated with the largest Lagrangian phenomena, generally called T_L and is comparable to the integral time in Eulerian statistics. If velocities are vertically correlated, i.e. for cases with dominant rotation, we do not expect the same mechanism to apply for a linear T-law. Although cases with rotation calculated by RDT/SCH exhibit a linear T-law and cases from KS and DNS show a short tendency toward a T-law at a time $T \approx 1$, this tendency is replaced in DNS and KS by a time law T^{γ}, with $\gamma \approx 2$, for $\alpha = \infty$. The linear evolution of rotating vertical single-particle dispersion may therefore not be due to an effect similar to Brownian diffusion as a random-walk evolution is expected to appear only at later times.

We observe further differences between the three cases. The oscillations in the linear method are regular and slowly damped, due to linear phase mixing only, which is not present at $\alpha = 1$(undamped oscillations). As a consequence, in DNS, the ascent of the one-particle dispersion seen for the case $\alpha = 1$ is a nonlinear effect. As the dynamics is strictly linear in KS, we attribute the similar evolution of the one-particle dispersion to the nonlinearity in the fluid trajectory equation (4). This "nonlinear" tendency of a reduced confinement is confirmed by KS and DNS runs at higher Froude numbers (not shown here).

2.2. Horizontal one-particle dispersion

Horizontal one-particle dispersion $\Delta_{11}(0,t)$ is shown in Fig. 3. Again, the similarity is good, though Fig. 3(a) and (c) from the linear method and DNS compare better than the KS results. As for Δ_{33}, in all three cases the horizontal one-particle dispersion shows a t^2 law at small times. With rotation one finds a linear t-law at about 0.1 integral time scales, which, depending on the amount of stratification, returns to a t^2 time evolution.

The main difference between the three figures is the vertical axis scaling, done here with the initial horizontal velocity correlation length scale $L_{11}^1 = \int \langle u_x(\boldsymbol{x}') \rangle \langle u_x(\boldsymbol{x}) \rangle \mathrm{d}x$, where $\boldsymbol{x}$ and $\boldsymbol{x}'$ differ by a strictly horizontal distance (Liechtenstein et al., 2005) and initial mean horizontal velocity $u_h^2 = (u_x^2 + u_y^2)/2$. The point of transition to anisotropic behaviour appears earlier in KS and latest in RDT/SCH. Furthermore, the transient linear t-law of DNS10 and

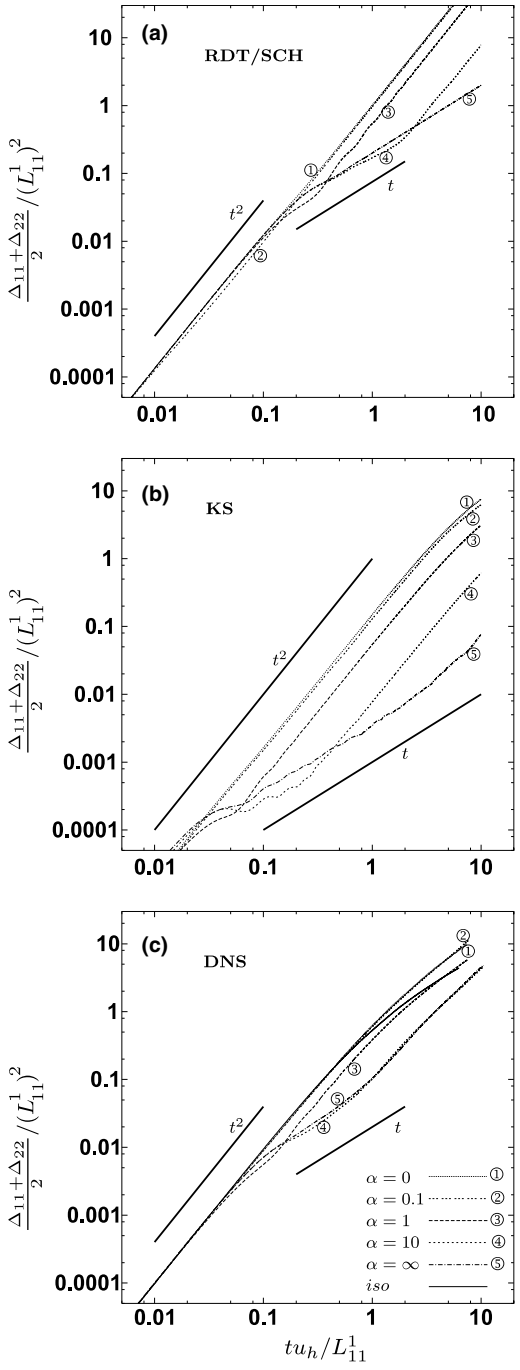

Fig. 3. (a) Linear prediction, (b) KS, and (c) DNS of horizontal one-particle dispersion for different $\alpha = 2\Omega/N$.

DNS-inf is not as long as the corresponding cases in RDT/SCH or KS. This might be a low Reynolds number effect as well as a difference between linear/nonlinear evolution.

Single-particle dispersion in isotropic turbulence exhibits a Brownian behaviour for very long times. This regime starts to appear in isotropic DNS shown in Fig. 3(c). All other runs do not show such a behaviour. In anisotropic turbulence the Brownian regime might still exist, but appearing only at longer times. The possible absence of a linear t-law for horizontal one-particle dispersion in anisotropic cases can be attributed to a non-zero velocity correlation length due to large structures. The long-time dynamic evolution of these as well as its relation to the Brownian regime is still unknown. KS has been reported to produce a Brownian regime for long times (Nicolleau and Vassilicos, 2000), though it cannot give a conclusive answer for a dynamically evolving flow field.

For pure rotation, the Brownian regime seems not to go back to a ballistic regime in RDT/SCH. Furthermore, the vertical diffusivity in this model is exactly twice the horizontal one (Cambon et al., 2004), a ratio which is only marginally recovered for the nonlinear data at intermediate times.

3. Two-particle dispersion

Two-particle dispersion is introduced by Richardson (1926) as the evolution of the distance from a fluid particle to an initially neighbouring one. It can be directly related to scalar diffusivity and so is the basic quantity in turbulent mixing.

For two particles $\boldsymbol{x}$ and $\boldsymbol{x}'$ the absolute two-particle dispersion is their separation squared $(\boldsymbol{x}(t) - \boldsymbol{x}'(t))^2$. It is calculated as a function of time and depends on the initial separation $\boldsymbol{\delta} = \boldsymbol{x}(0) - \boldsymbol{x}'(0)$. The relative two-particle dispersion Λ is defined as $\Lambda_{ii}(t) = \langle x_i(t) - x_i'(t)\rangle^2 - \delta_i^2$. No relation as easy as Taylor's relation for single-particle dispersion can be found, as two trajectories and the history of velocity correlations of the two trajectories are involved. Therefore, analytical models for two-particle dispersions are rare. We therefore only use KS and DNS for the calculation of Λ, no analytical or RDT/SCH model is presented.

We analyse exclusively the relative two-particle dispersion, as the initial evolution of the separation is so small that it cannot be observed in the absolute two-particle dispersion. The initial separation of the runs from KS and DNS is comparable and amounts to about half a Kolmogorov length scale η. As for single-particle dispersion, two-particle dispersion in anisotropic turbulence depends strongly on the direction, so we calculate Λ_{ii} separately for the vertical and horizontal directions.

3.1. Vertical two-particle dispersion

Vertical two-particle dispersion is shown in Fig. 4, calculated with KS and DNS. A basic similarity between the two curves exists in an initial *ballistic* separation, an intermediate *transition* and a *final* fast separation $\propto t^2$ for dominantly stratified cases to a very fast separation $\propto t^3$ for dominantly rotating cases. However, the similarity between KS and DNS is not as complete as for the single-particle dispersion, illustrated by the difference in scales for Fig. 4(a) and (b). This is in contrast with Fig. 2.

The vertical scalings in the graphs is similar to the one used for single-particle separation multiplied by δ^2 in units of the Kolmogorov length scale η. With this scaling, all curves of KS collapse in the ballistic regime with a

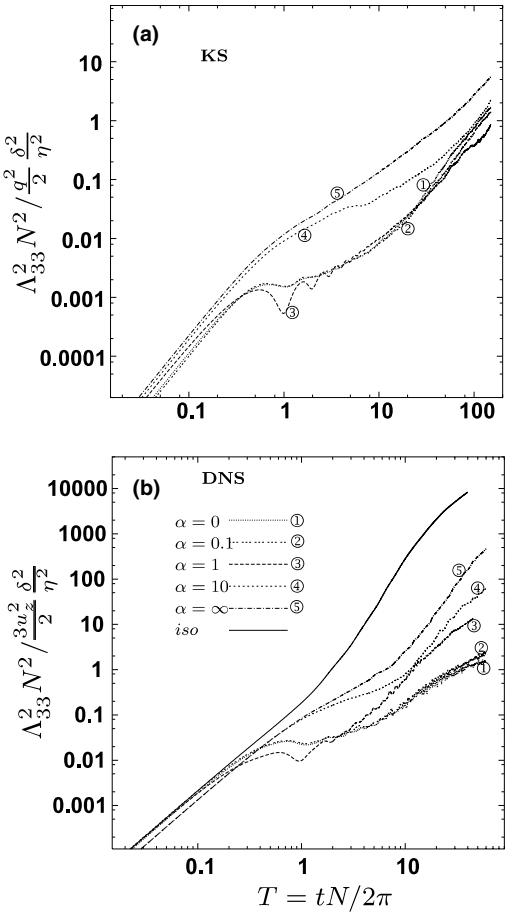

Fig. 4. (a) KS and (b) DNS of vertical two-particle dispersion for different $\alpha = 2\Omega/N$. The dominantly rotating curves are scaled with 2Ω instead of N for the time as well as the dispersion scale.

transition occurring at around $T = 0.5$ and normalized $\Lambda_{33}^2 = 0.02$. The collapse of the ballistic regime in DNS is less good. However, the transition occurs at approximately the same $T = 0.5$ and normalized $\Lambda_{33}^2 = 0.02$ as in KS. After the transition, DNS exhibits oscillations at the Brunt–Vaisala frequency for DNS1, a very short plateau for DNS0 and DNS0.1, and slower separation rates than t^2 for DNS10 and DNS-inf. The transition of KS shows qualitatively the same features, although less pronounced. This can be an effect of the absence of a nonlinear flow field in KS. Moreover, as two-particle dispersion depends on the history of trajectories, the fundamental difference of a non-decaying flow field in KS and a freely decaying one in DNS might also explain some differences. This suggests an increased importance of the dynamics of the flow field for two-particle compared to single-particle Lagrangian statistics.

KS with parameters comparable to DNS generally show a reduced plateau due to the absence of coherent structures in KS fields. As dominantly stratified turbulence has strong horizontal vorticity, two particles at approximately the same height, but horizontally apart, will be in two different horizontal vortex structures. So their vertical two-particle dispersion oscillates around a plateau, the size of which is connected to the size of the structures. A recent topological argument for this in Dávila and Vassilicos (2003) relates stagnation points to particle separation. The size of the structures indeed seems to play an important role in the plateau of DNS, as preliminary results of further simulations show, when trajectories for two-particle dispersion are started at significantly later times. Due to the decay of turbulence, the velocity field at this time has both less energy and a larger turbulent turnover time, producing a more stable flow field, which vertically de-correlates the two particles less fast.

Contrary to Nicolleau and Vassilicos (2000), a second plateau is not observed in dominantly stratified KS. This is not necessarily contradictory, as they used Froude numbers of 0.0034, while in this work Froude numbers are of the order of 0.05. Our KS and DNS at lower Froude numbers exhibit this second plateau (not shown). The length of the plateau is indeed not only dependent on the size of coherent structures, but also on the Froude number (Nicolleau and Vassilicos, 2000).

The structure formation might also explain the comparatively slow long-time separation of the cases DNS0 and DNS0.1 compared to the case DNS1. The coherent structures are strongly formed for dominant stratification while nearly nonexistent for DNS1. As no coherent structures can be formed in KS, the dominantly stratified cases will undergo the same linear processes as case KS1 and so evolve similarly. However, this also means that a plateau observed in DNS potentially created by a distribution of structures, and a plateau observed in KS because of a strong confinement in the vertical are qualitatively different, the latter only being linearly driven buoyancy oscillations.

The final period of evolution of two-particle dispersion shows the most distinct differences between KS and DNS, showing the increasing importance of nonlinear dynamics with time. KS exhibits a very fast growing separation with a rate of t^3 and more for all parameters. The cases KS0 and KS0.1 actually show a relative vertical separation which is larger than the one from cases KS10 and KSinf. In DNS we observe separation rates between t and t^2 for cases DNS0, DNS0.1 and DNS10 and slightly higher for cases DNS1 and DNS-inf. Neither a Brownian regime nor absolute values close to single-particle separation are observed for any of the cases at longest times. Furthermore, no second plateau is observed for the two-particle dispersion in the dominantly stratified cases. This might be due to too short integration times.

3.2. Horizontal two-particle dispersion

Horizontal two-particle dispersion is shown in Fig. 5(a) for KS and Fig. 5(b) for DNS. A basic qualitative similarity can be detected, which shows an initial ballistic behaviour and certain qualitative changes in the rate of separation at longer times.

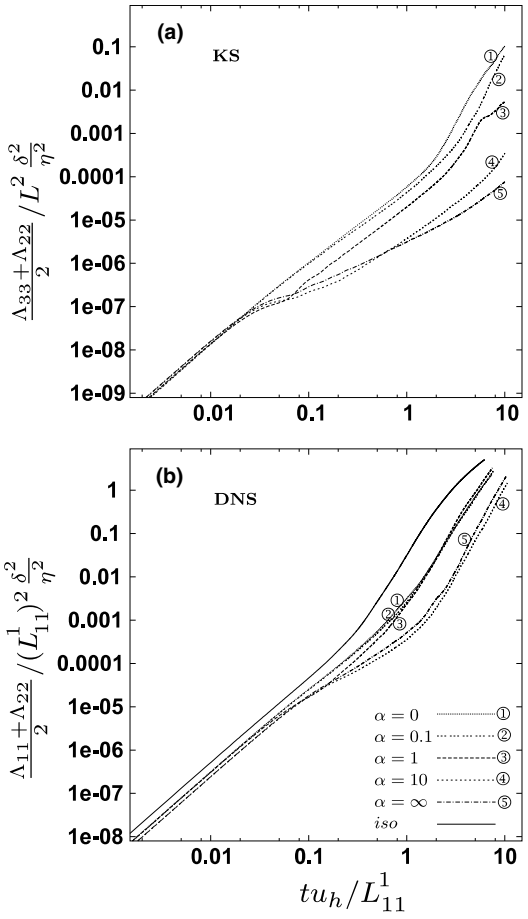

Fig. 5. (a) KS and (b) DNS of horizontal two-particle dispersion for different $\alpha = 2\Omega/N$.

The KS runs show an excellent agreement in the scaling of the ballistic regime. A transition occurs at around $tu_h/L_{11}^1 = 0.1$, where the dominantly stratified cases KS0 and KS0.l follow an evolution close to isotropic two-particle dispersion. This means that a quasi-inertial range is observed with a separation rate close to t^3 at times $1 < tu_h/L_{11}^1 < 10$ followed by an evolution which tangentially approaches a Brownian t-law.

The cases KS1, KS10 and KSinf show a different long-time evolution. They exhibit a t-law for times $0.1 < tu_h/L_{11}^1 < 10$, which cannot be of Brownian origin, as the trajectories are not de-correlated yet. The physical principle of the slowed down rate of separation is yet unknown, but possibly connected to similar observations concerning single-particle dispersion. A transition to a t^3-law or faster dispersion is seen at later times. The purely rotating case undergoes this transition at around $tu_h/L_{11}^1 = 20$. The cases KS1 and KS10 exhibit a shorter range for the t-law, then evolving parallel to the dominantly stratified cases, although at a lower absolute value.

In Fig. 5 for DNS we see the initial ballistic regime for all parameters. Compared to KS, the ballistic regime changes to a transition region at significantly later times. In the transition region, the cases DNS10 and DNS-inf follow a linear t-law evolution for a short time. At $tu_h/L_{11}^1 \approx 2$ all runs exhibit a t^3-law, much later than in the isotropic run. A slightly slower separation is observed for cases with rotation due to the earlier linear evolution. Furthermore, contrary to the evolution of cases KS10 and KSinf, DNS10 and DNS-inf evolve very similarly. No Brownian regime is observed for long times, possibly due to too short integration times.

3.3. KS of two-particle dispersion

From the foregoing discussion we deduce an important impact of nonlinear mechanisms on two-particle dispersion, notably larger than for single-particle dispersion. The KS presented here seem to not model the nonlinear mechanisms with the needed precision to predict two-particle dispersion in rotating and stratified turbulence. So do we need to abandon the idea of using KS-like models based on linear dynamics to predict two-particle dispersion statistics? Not necessarily, as the KS presented here can be modified to maybe capture nonlinear phenomena. Effects of nonlinearity can be generated in two ways. The first way is by introducing a stochastic or semi-stochastic time-dependency of the initial wave vectors, which could simulate the slow nonlinear evolution of the flow field in Fourier space (Nicolleau and Vassilicos, 2000; Fung et al., 1992). The second way is to modify the initialization. The initial energy spectrum is the most important ingredient in simulating the nonlinear phenomena in the KS. As to our knowledge the anisotropic spectral structure of the energy density of rotating and stratified turbulence is not yet known, the initial spectrum of the KS is in its best case an approximation. Furthermore, the details of initializing a 3D-flow field by choosing random Fourier modes can influence the final velocity field significantly. We therefore believe that the two-particle dispersion of the KS can be significantly improved by more detailed information of Eulerian statistics, in particular of the spectral energy density distribution, of rotating and stratified turbulence.

4. Conclusions

4.1. Lagrangian statistics of rotating and stratified turbulence

Particle trajectories in purely stratified turbulence are confined to a vertical level for very long times as shown by stochastic models (Csanady, 1964), DNS (Kimura and Herring, 1996), KS (Nicolleau and Vassilicos, 2000), linear models (Kaneda and Ishida, 2000) or experiments (Britter et al., 1983), even for weakly stratified turbulence. The trajectories are oscillating and bounded by the potential energy. Vertical single-particle dispersion in purely stratified turbulence therefore exhibits damped oscillations forming a plateau, after an initial ballistic regime. The plateau is easily related to the finite potential energy reservoir in the system. However, the various studies with the different techniques do not agree with each other on the

evolution of the damped oscillations and do not estimate the long-time evolution of vertical single-particle dispersion. The horizontal single-particle dispersion is often assumed to be similar to isotropic dispersion. However, we find quantitative differences for some of the horizontal statistics.

In rotating turbulence no potential energy is available and the particle dispersion is qualitatively similar to isotropic turbulence. Slight qualitative differences, namely a factor two between horizontal and vertical dispersion, are found with a linear model (Cambon et al., 2004).

4.2. The role of nonlinearity in Lagrangian statistics

There is a paradox. In a stratified fluid the layering or pancake dynamics, observed when looking at velocity snapshots (Liechtenstein et al., 2005) or single-time Eulerian statistics, is a nonlinear phenomenon, at least for homogeneous turbulence. How can linear theory predict anisotropy of turbulent trajectories in two-time statistics? This applies also to rotating turbulence.

Due to the lack of anisotropy in a linearly generated flow field (Liechtenstein et al., 2005), Lagrangian statistics include anisotropy of the flow field exclusively through the trajectory equation, whose nonlinearity might be a substitute for the nonlinear advection term in the Navier–Stokes equation. Over the Taylor hypothesis, this also applies for two-time statistics of RDT/SCH. If this is true, then Lagrangian statistics altered by instantaneous structures, such as two-particle statistics should be influenced significantly by the absence of a nonlinear term in the dynamical evolution of the flow field. This is partly confirmed by a different scaling in two-particle dispersion, without final conclusive answers provided by KS or DNS. To be able to follow up on this problem, a two-particle two-time RDT velocity correlation model is needed.

Although universal scaling laws have been found for different Lagrangian statistics, linear and nonlinear models scale differently because of the different degrees of anisotropy in their respective Eulerian statistics. This is a definite influence of nonlinear dynamics of the Eulerian field on Lagrangian statistics, not included in either KS or RDT/SCH. DNS results show a nonlinear development of the velocity fields with distinct anisotropies and structures formed, which depend on α. The connection between coherent structures in instantaneous Eulerian fields and trajectories is, therefore, evidently not possible without nonlinearities in the flow field. This questions previous empirical attempts to connect Eulerian and Lagrangian length scales, and suggests to revisit the existing scalings, with a particular emphasis on the directional Eulerian statistics.

To achieve this goal, a Lagrangian parametric study using DNS of rotating and stratified turbulence is needed. Due to the long simulation times needed to generate quality Lagrangian data, this involves a continuous cooperation with supercomputing centers, and we therefore want to thank equally IDRIS (computing center of French CNRS) and CCRT (computing center of French CEA).

References

Britter, R.E., Hunt, J.C.R., Marsh, G.L., Snyder, W.H., 1983. J. Fluid Mech. 127, 27–44.
Cambon, C., Scott, J.F., 1999. Annu. Rev. Fluid Mech. 31, 1–53.
Cambon, C., Godeferd, F.S., Nicolleau, F., Vassilicos, J.-C., 2004. J. Fluid Mech. 499, 231–255.
Corrsin, S., 1963. J. Atmos. Sci. 20, 115–119.
Csanady, G.T., 1964. Turbulent diffusion in a stratified fluid. J. Atmos. Sci. 21, 439–447.
Dávila, J., Vassilicos, J.C., 2003. Phys. Rev. Lett. 91 (14).
Fung, J.C.H., Hunt, J.C.R., Malik, N.A., Perkins, R.J., 1992. J. Fluid Mech. 236, 281–318.
Kaneda, Y., Ishida, T., 2000. J. Fluid Mech. 402, 311–327.
Kimura, Y., Herring, J.R., 1996. J. Fluid Mech. 328, 253–269.
Liechtenstein, L., Godeferd, F.S., Cambon, C., 2005. J. Turb. 6.
Nicolleau, F., Vassilicos, J.C., 2000. J. Fluid Mech. 410, 123–146.
Richardson, L.F., 1926. Proc. Roy. Soc. A 110, 709.
Rogallo, R.S., 1981. Numerical experiments in homogeneous turbulence. NASA Tech. Mem. 81315.
Taylor, G.I., 1921. Proc. London Math. Soc., Ser. 2 20, 196–211.